

Spin Isomers of the Shape Isomer $^{237m}\text{Pu}^\dagger$

P. A. Russo, R. Vandenbosch, M. Mehta,* J. R. Tesmer, and K. L. Wolf‡

University of Washington, Seattle, Washington 98105

(Received 23 December 1970)

Two components in the spontaneous-fission decay of ^{237m}Pu have been investigated. The half-lives of the two isomers are 82 ± 8 nsec and 1120 ± 80 nsec. The production ratio of the two components was determined for three different bombarding conditions: $^{235}\text{U} + 24\text{-MeV } \alpha$ particles, $^{235}\text{U} + 27\text{-MeV } \alpha$ particles, and $^{237}\text{Np} + 12.1\text{-MeV}$ deuterons. The dependence of the production ratio on angular momentum deposition for the various reactions shows that the two shape isomers differ in spin, with the short-lived component corresponding to the lower-spin state. The experimental isomer ratios are compared with statistical-model calculations. Assuming the validity of the statistical description of isomer population, and the absence of a significant γ -decay branch for the high-spin isomer, the deformation associated with shape isomerism can be deduced from isomer-spin information extracted from the present experiment and reference to the Nilsson diagram at large deformation. The deformation indicated is approximately $\epsilon = 0.6$, in good agreement with theoretical estimates.

I. INTRODUCTION

Spontaneous-fission isomerism is believed to be a consequence of a double-humped fission barrier,^{1,2} with the short-lived isomeric states at a deformation approximately twice the equilibrium ground-state deformation. The lifetime of the lowest state in the second well is determined by the penetrability of the outer barrier to fission, or possibly by penetrability of the inner barrier to γ decay to the normal ground state. Only the first type of decay has been experimentally observed although measured spontaneous-fission lifetimes may in some cases reflect the lifetime for γ decay back to the ground state.

A nucleus with a deformation corresponding to that of a shape isomer is expected to exhibit an energy-level spectrum similar to that of nuclei with normal deformations. For even-even nuclei, the lowest states will be rotational in character and will have energies of only 10's of keV. If a nucleon pair is broken, two quasiparticle states with excitation energies of the order of 1 MeV above the lowest shape-isomeric state are expected. It has been suggested³⁻⁵ that the spontaneous-fission isomers ^{236}Pu and ^{238}Pu , characterized by abnormally long lifetimes, high-excitation energies, and low yields, are two-quasiparticle states whose lifetimes with respect to γ decay (without shape change) to the lowest state of the shape-isomeric well are comparable to the fission lifetimes. For these nuclei, the half-life of the lowest state of the second minimum is expected to be too short to have been observed by presently available techniques.

Fairly close-lying single-particle states, each with its own rotational band, are expected for odd-*A* shape-isomeric nuclei. A fairly small energy

difference or a sizable spin difference between two single-particle states may result in spin isomerism for high deformations just as for ground-state deformations. The spontaneous-fission lifetimes may be rather different even for two single-particle states fairly close in energy because of the possibility of very different specialization energies⁶⁻⁸ for the two states. The implications of specialization energy for shape isomers has been recently discussed by Wolf.⁶

The present work is an outgrowth of earlier experiments which indicated the possibility of more than one isomer in the odd-*A* nucleus ^{237}Pu . The aim of this work was to confirm the existence of multiple isomerism in ^{237}Pu and to characterize the isomers as fully as possible. It is of particular interest to correlate the different half-lives with differing spin states and to identify which component has the higher spin. A more definitive characterization of the spins would present the interesting possibility of identifying specific Nilsson single-particle states at the deformation corresponding to the second minimum of the potential-energy curve. Such an identification would provide a crucial test of theoretical calculations of the double-humped barrier.

II. EXPERIMENTAL PROCEDURE

The ^{237m}Pu fission isomers were produced by bombardment of ^{236}U with α particles from the University of Washington 60-in. cyclotron, and by bombardment of ^{235}U and ^{237}Np with chopped beams of α particles and deuterons, respectively, from the University of Washington two-stage tandem Van de Graaff accelerator.

The targets, 200 to 500 $\mu\text{g}/\text{cm}^2$ thick, were prepared by molecular plating the fissionable materi-

al onto 150- $\mu\text{g}/\text{cm}^2$ copper-backed nickel and then by etching off the copper.

The delayed-fission events were identified electronically. Time spectra were obtained by measurement of the time interval between the arrival of a beam burst and the detection of a delayed-fission event. A time-to-amplitude converter was started by the fast signal from a semiconductor fission detector and stopped by a signal from the cyclotron oscillator or Van de Graaff beam chopper to obtain a time spectrum of fission fragments. For each delayed event, independent time measurements were obtained from each of two semiconductor fission detectors located 180° apart and separated by less than 5 cm. A four-fold coincidence among the fast and slow energy-analyzed signals from the two detectors provided a gate to the computer or, in the case of the cyclotron experiment, to a 1024-channel analyzer in which the

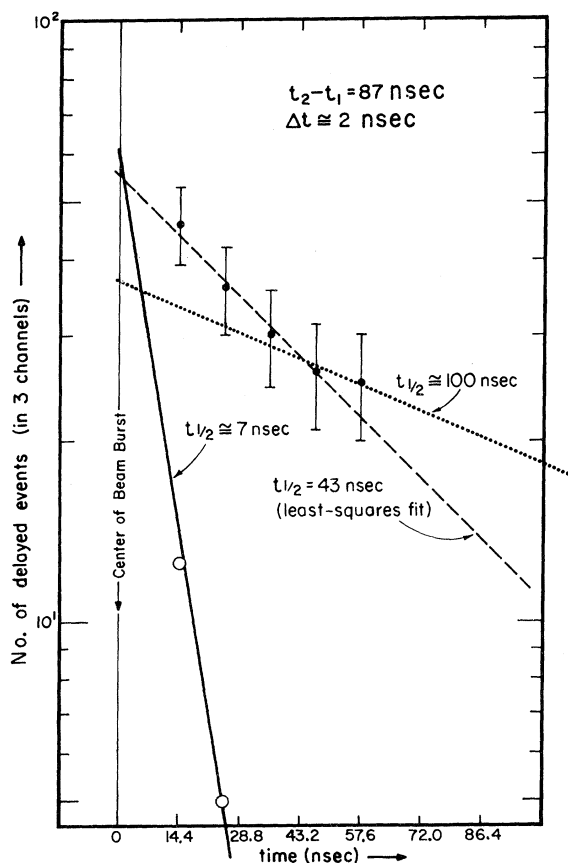


FIG. 1. Decay curve resulting from 34-MeV α bombardment of ^{236}U . The dotted 100-nsec line is arbitrarily drawn to fit the longer-lived decay. The dashed 43-nsec line is a least-squares fit to all the data. The open circles were obtained by subtracting the 100-nsec line from the data points. The solid 7-nsec line is arbitrarily drawn to fit the open circles.

time spectra were stored as two-dimensional arrays. Decay curves were constructed from coincident events along the diagonal of the array. The method has been described elsewhere in greater detail.^{3,6}

The deuteron beam from the direct-extraction negative-ion source on the tandem was chopped and bunched^{6,9} for the first time during these experiments. Prompt-fission background between deuteron beam bursts observed with previous operation of the duoplasmatron negative-ion source¹⁰ was not detected in these experiments with the direct-extraction source. Prompt-fission background between α beam bursts was also absent in these experiments. The background is determined by using a ^{232}Th target as described elsewhere.⁶

An electronic effect first observed during one of the Van de Graaff α -particle experiments was eventually attributed to the use of crossover timing in the slow electronics at high count rates for the scattered α particles. The observed symptom of this effect was a small loss of delayed events in a narrow time interval approximately 1 μsec after the beam burst. The effect was diagnosed by pulser tests with beam on target, and was attributed to a reduction to subdiscriminator amplitude of the lower-energy fission-fragment amplifier signals caused by the simultaneous occurrence of the negative part of a bipolar energy signal from a scattered α particle and the positive part of a comparable signal from a fission fragment at the lower end of the energy spectrum. Further tests defined the time region affected and this region was excluded in subsequent data analysis. The results are therefore not affected.

III. RESULTS

A. Search for Component with a Very Short Lifetime

The 60-in. cyclotron, with 87-nsec intervals between beam bursts of approximately 2-nsec duration, was used to investigate a reported⁶ short-lived (35-nsec) component in the time spectrum of delayed fissions resulting from the 34-MeV α -particle bombardment of ^{236}U . An aluminum degrader was used to achieve this energy.

The excitation function for the $(\alpha, 3n)$ reaction peaks near 34 MeV. The decay curve for delayed fission appears in Fig. 1 and the linear least-squares fit gives a half-life of 43 nsec. However, subtraction of a line with a 100-nsec half-life drawn through the points at the end of the time spectrum results in a decay corresponding to a half-life of approximately 7 nsec. The 100-nsec component has been previously identified⁶ as a decay resulting from the formation of ^{237m}Pu .

Experiments by Burnett *et al.*⁴ report a 6.5-nsec

half-life for the fission isomer ^{238m}Pu suggesting that the short lifetime observed in the present experiment could be the result of the $(\alpha, 2n)$ reaction to form ^{238m}Pu instead of ^{237m}Pu . Estimates of the expected contribution of ^{238m}Pu from spallation data¹¹ and isomer ratios⁴ are qualitatively consistent with the relative amounts of short- and longer-lived activity in Fig. 1. The very large uncertainty is due to the very poor statistics of the decay curve.

If the 7-nsec component of the α data is ^{238m}Pu , then bombardment of ^{237}Np with deuterons giving an excitation energy comparable to that in the α experiment should produce no 7-nsec component. The reactions $^{237}\text{Np}(d, 2n)$ and $^{237}\text{Np}(d, n)$ will both occur, but the latter proceeds largely by a direct mechanism and should contribute little to the production of fission isomers.^{10, 12}

Figure 2 shows the time decay resulting from the experiment performed with a chopped and bunched beam of 12.1-MeV deuterons from the Van de Graaff incident on a ^{237}Np target. The beam bursts were 3 nsec wide (full width at half maximum) at 335-nsec intervals. The short-lived component does not appear here and is attributed,

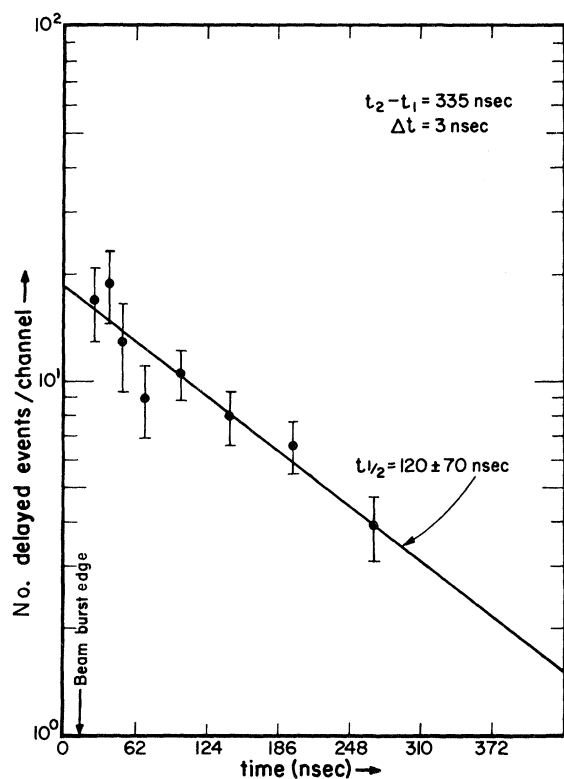


FIG. 2. Decay curve resulting from 12.1-MeV deuteron bombardment of ^{237}Np with short time intervals (335 nsec) between narrow beam bursts. The solid line is a least-squares fit to the data.

therefore, to ^{238m}Pu .

B. Identification of the ^{237m}Pu Isomer (Excitation Function)

The Van de Graaff α beam was chopped and bunched to a 40-nsec-wide beam burst at 400-nsec intervals to identify the component with a half-life near 100 nsec. An excitation function was taken under these conditions with incident α -particle laboratory energies of 24 to 27 MeV. This is shown in Fig. 3 which is a plot of the ratio of the number of delayed fissions to the total integrated beam. The peak between 25 and 26 MeV is indicative of the $(\alpha, 2n)$ reaction.

Figure 4 shows the corresponding decay curve for delayed fission (solid points) and includes data taken over the entire energy range. A linear least-squares fit to these data give a half-life of 108 ± 9 nsec, in agreement with other measurements.^{4, 6}

C. Investigation and Characterization of Long and Short Components

The reported¹³ appearance of a longer-lived com-

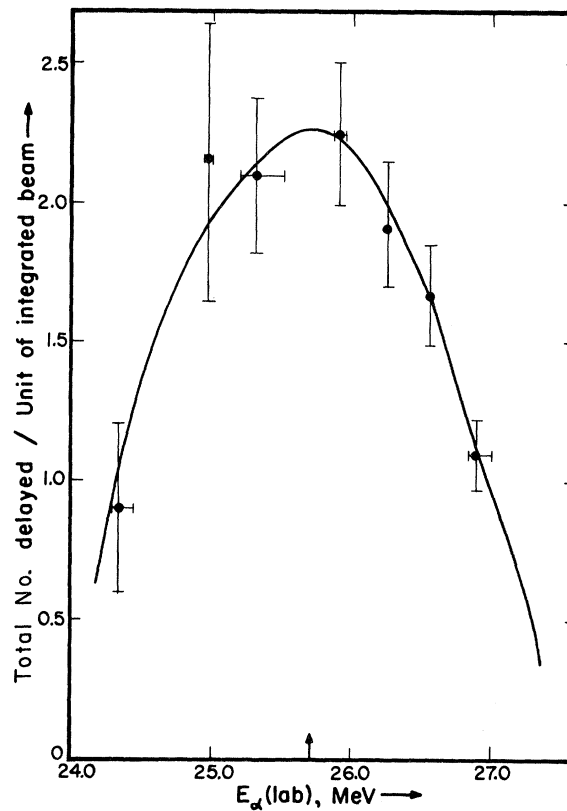


FIG. 3. Excitation function for the reaction $^{235}\text{U}(\alpha, 2n)-^{237m}\text{Pu}$ taken with 400-nsec intervals between α beam bursts. Data include all delayed events observed between $t = 70$ and 300 nsec in the interval between beam bursts.

ponent in ^{237m}Pu led to further investigations which used the chopped Van de Graaff beam with intervals between beam bursts (3.0- to 3.6- μsec intervals between 250- and 350-nsec-wide bursts) sufficiently long to simultaneously observe the 100-nsec component and the longer-lived decay. To determine the effect of angular momentum on the relative isomer yields, different initial compound-nuclear-spin distributions were obtained by varying the energy and mass of the projectile. Experiments were performed with 24- and 27-MeV α particles incident on ^{235}U and 12.1-MeV deuterons on ^{237}Np . The two-component decay curve for the 12.1-MeV deuteron case is shown in Fig. 5. This was obtained by projecting the 64-by-128-channel two-dimensional time spectrum onto the 64-channel side. A similar projection onto the 128-channel side gave a second determination based on the independent timing information of the complementary fragment in the second detector. The data

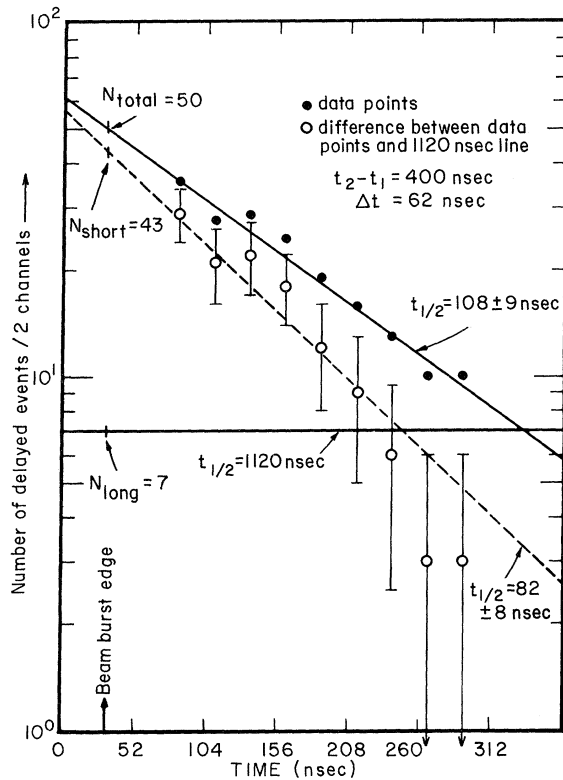


FIG. 4. Decay curves for the short-lived component of ^{237m}Pu . Solid points are data points for the 24-27-MeV α bombardment of ^{235}U . The 108 ± 9 -nsec line is the least-squares fit to these points. The 1120-nsec line is the contribution of the long-lived component to the data. The open circles were obtained by subtracting the 1120-nsec line from the data (solid) points. The error bars on the open circles are equal in magnitude to the statistical errors in the corresponding data points. The dashed line is a weighted least-squares fit to the open circles.

for each of the three bombardments was treated in this manner.

The half-lives determined by resolving the long- and short-lived components and separately fitting each component to a straight line are summarized together with the statistical errors in Table I. Agreement within error is observed in the results for the long-lived component whose mean lifetime, from a weighted average of the values in Table I, is 1120 ± 80 nsec.

The positions in time of the points used to determine the half-life of the short-lived component were corrected for channel width. The errors in these points are fractionally large due to the subtraction of the long-lived component. The weighted mean half-life of the short-lived component is 88 ± 33 nsec.

The relative cross sections for production of the long- and short-lived components were determined with the expression:

$$\sigma_i \propto N_i / (1 - e^{-\lambda_i \Delta t}),$$

where σ_i is the cross section of the i th component,

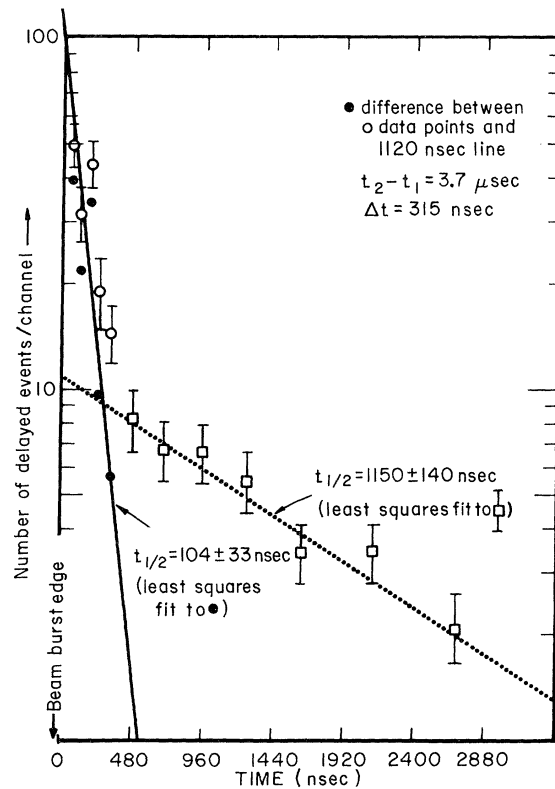


FIG. 5. Two-component decay curve of ^{237m}Pu from the 12.1-MeV deuteron bombardment of ^{237}Np with long time intervals (3.7 μsec) between beam bursts. The 1150 ± 140 -nsec dotted line is the least-squares fit to the short-lived points after subtraction of the long-lived contribution.

TABLE I. Experimental half-lives of ^{237m}Pu .

Incident particle	$t_{1/2}$ short (nsec)	$t_{1/2}$ long (nsec)
12.1-MeV deuterons	104 ± 33 (64-channel side)	1150 ± 140 (64-channel side)
	120 ± 35 (128-channel side)	1190 ± 380 (128-channel side)
24-MeV α particles	128 ± 9 (64-channel side)	940 ± 190 (64-channel side)
	126 ± 13 (128-channel side)	1100 ± 290 (128-channel side)
27-MeV α particles	100 ± 7 (64-channel side)	1175 ± 110 (64-channel side)
	57.6 ± 2 (128-channel side)	1090 ± 290 (128-channel side)
Weighted mean	88 ± 35	1120 ± 80

N_i is the number of decays per unit time for the i th component at the edge of the beam burst, λ_i is the decay constant for the i th component, and Δt is the width of the beam burst. The edge of the beam burst is taken to be the half maximum, and N_i is the vertical intercept, corrected for the contribution from the previous beam burst, in the time spectrum at this position.

The mean half-lives given in Table I for the long and short components were used to determine N_L and N_S from which σ_i and σ_S were evaluated. The mean result of σ_S/σ_L for the two α experiments was used to reevaluate the half-life of the short-lived component from the data (solid points) of Fig. 4 by subtracting off the long-lived component to give the open circles in Fig. 4. The new decay curve appears as the dashed line of Fig. 4, a least-squares fit to the open circles and results in a half-life of 82 ± 8 nsec. A compromise half-life of 85 nsec was used to reevaluate σ_L and σ_S for the three cases. The ratios, σ_S/σ_L , are summarized in Table II. The errors are due to the statistical error in N_S (evaluated from a least-squares fit of the short-lived data to an 85-nsec decay), the intercept at the beam burst edge for the short-lived component. The ratios of delayed fission to prompt fission and of delayed fission to spallation are given in Table III.

IV. DISCUSSION

As the angular momentum brought in by the incident particle increases, the population of final

states shifts to higher spins. The experimental values of $\sigma_{\text{short}}/\sigma_{\text{long}}$ in Table II decrease with increasing angular momentum showing that the short-lived (85-nsec) component of ^{237m}Pu is the lower angular momentum state. The excitation energy in the compound nucleus ^{239}Pu is exactly the same for 12.1-MeV deuterons on ^{237}Np as for 27-MeV α particles on ^{235}U . Thus, the observed effect cannot be attributed to an energetic effect which might arise if the two isomers had sufficiently different excitation energy, and must be attributed to angular momentum. Although there is evidence from this experiment that the two isomers differ in spin, it is not possible to conclude that the two isomers have the same shape. The isomers could correspond to two different shapes separated by a barrier in deformation space. The following discussion will proceed on the assumption that the two isomers have essentially the same deformation. The difference in half-life of more than an order of magnitude has several possible explanations. The high-spin isomer may have a longer half-life because it lies lower in energy than the low-spin isomer. The required energy difference is only a few tenths of an MeV. The half-life differences may also be a consequence of another mode of decay such as γ decay from one of the isomeric states to the ground state. This does not seem probable because of the high absolute yields of both isomers. A likely explanation is that the specialization energies are different for the two spin states resulting in different barrier heights. It is not surprising that the long-lived isomer has the

TABLE II. Production ratios of the ^{237m}Pu isomers for reactions with different mean square initial compound-nuclear spin \bar{J}_C^2 .

Incident particle	\bar{J}_C^2 Compound nucleus	σ_S/σ_L (64-channel side) (%)	σ_S/σ_L (128-channel side) (%)	σ_S/σ_L (weighted mean)
12.1-MeV deuterons	15	1.8 ± 39	1.6 ± 29	1.7 ± 0.6
24-MeV α particles	27	1.27 ± 26	0.99 ± 43	1.13 ± 0.39
27-MeV α particles	53	0.71 ± 26	0.77 ± 45	0.74 ± 0.26

TABLE III. Isomer ratios for ^{237m}Pu .

Target	Projectile	$\frac{\sigma_{\text{long}}}{\sigma_{\text{prompt}}}$ (10^{-6})	$\frac{\sigma_{\text{short}}}{\sigma_{\text{prompt}}}$ (10^{-6})	$\frac{\sigma_{\text{delayed}}}{\sigma_{\text{prompt}}}$ (10^{-6})	$\frac{\sigma_{\text{delayed}}}{\sigma_{\text{spallation}}}$ (10^{-6})
^{235}U	24-MeV α particles	5.61	6.3 ± 3.2	11.9 ± 3.2	300 ± 60
^{235}U	27-MeV α particles	2.65	1.9 ± 0.9	4.5 ± 0.9	180 ± 40
^{237}Np	12.1-MeV deuterons	2.59	4.5 ± 1.9	7.1 ± 1.9	

higher spin, especially if the spin is $I = \frac{11}{2}^-$, a possibility suggested below.

The ratio of the total yield of delayed fission to that of prompt fission, $\sigma_{\text{delayed}}/\sigma_{\text{prompt}}$ for the 27-MeV α case is about 30% less than the same ratio for the 12.1-MeV deuteron case, although the numbers agree within their experimental uncertainties. At an excitation energy of the order of the barrier energy, the ratio of the level density for high-spin states at the ground-state deformation to the level density for high-spin states at the isomer deformation is larger than the average level-density ratio at this excitation energy. This should decrease the delayed-to-prompt yield ratio resulting from the α bombardment compared to the deuteron bombardment with identical excitation energy due to the higher incident angular momentum of the α particles. A calculation indicates an expected difference of about 7% due to this effect.

The reactions used to determine the ratios given in Table II both lead to the same final nucleus from the same initial compound nucleus. The spin distribution of the initial compound nucleus, $P(J_C)$, depends upon the target and projectile spins and on the momentum of the incoming projectile. The final-spin distribution, $P(J_F)$, of the residual nucleus after neutron evaporation and deexcitation by γ emission depends upon the initial compound-nuclear spin distribution and on the angular momentum carried away by neutrons and γ rays prior to the final transition populating either of the isomeric states. Calculation of the final-spin distribution has been carried out with a formalism^{14, 15} and computer program¹⁶ described elsewhere. The compound-nuclear spin distribution is obtained by appropriate weighting of the transmission coefficients of the incoming projectile according to the coupling of target and projectile spins. The spin distribution after each particle emission is obtained by weighting a sum over transmission coefficients with an expression for the density of final states. A similar weighting is done for the dipole γ ray assumed to be emitted prior to the final nonstatistical transition(s) leading to final population of the isomer. Transmission coefficients for α particles and deuterons were obtained from optical-model calculations¹⁷ ignoring spin-orbit coupling between the deuteron and the target

nucleus. Calculations were performed with two different values of the spin cutoff parameter, σ , which enters in the density of states expression. $P(J_F)$ was calculated for each case with $\sigma = 3$ and 5. This covers the typical range of spin-cutoff parameters required in fitting isomers of known spin.¹⁸⁻²⁰

The calculated distribution of final states was used to determine the theoretical production ratio of any two final spin states which are genetically unrelated by integrating the appropriate portion of the spin distribution based on the assumption that a given spin state will feed the isomer whose spin is closest to it. This assumption is open to question because of the likelihood of nonstatistical effects in the γ cascade feeding the isomer states, particularly in the rotational bands. To a certain extent, this is probably accounted for by the use of empirical spin-distribution parameters. The theoretical isomer ratio, the ratio of the yield of the low-spin-to-high-spin state is plotted, along with the experimental values of $\sigma_{\text{short}}/\sigma_{\text{long}}$, for each combination of final-state spins from $\frac{1}{2}$ to $\frac{11}{2}$ vs the mean square value of the initial compound-nuclear spin distribution. The graphs for $\sigma = 3$ and 5 appear in Figs. 6(a) and 6(b), respectively.

Figure 7 is a plot of the calculated and experimental values of the ratio of each of the three isomer ratios to the isomer ratio for the 27-MeV α bombardment plotted against the mean square value of the initial compound-nuclear spin distribution. The calculated values selected were for the spin pairs $\frac{3}{2}, \frac{11}{2}$, and $\frac{5}{2}, \frac{9}{2}$, since these lie at the experimental limits according to the graph in Fig. 6(a). The experimental results behave much like the calculations in spite of the large error bars. In fact, such plots for all other spin pairs are very similar to the curves shown, and all lie within the limits of experimental error. This apparent insensitivity of the ratio of isomer ratios to the isomer spins assumed is simply a consequence of the similarity in the slopes of the curves in Fig. 6. The insensitivity of the calculated ratios of isomer ratios to the statistical parameters and the good agreement with the experimental values supports the assumption that the variation in isomer ratios in the three bombardments is directly re-

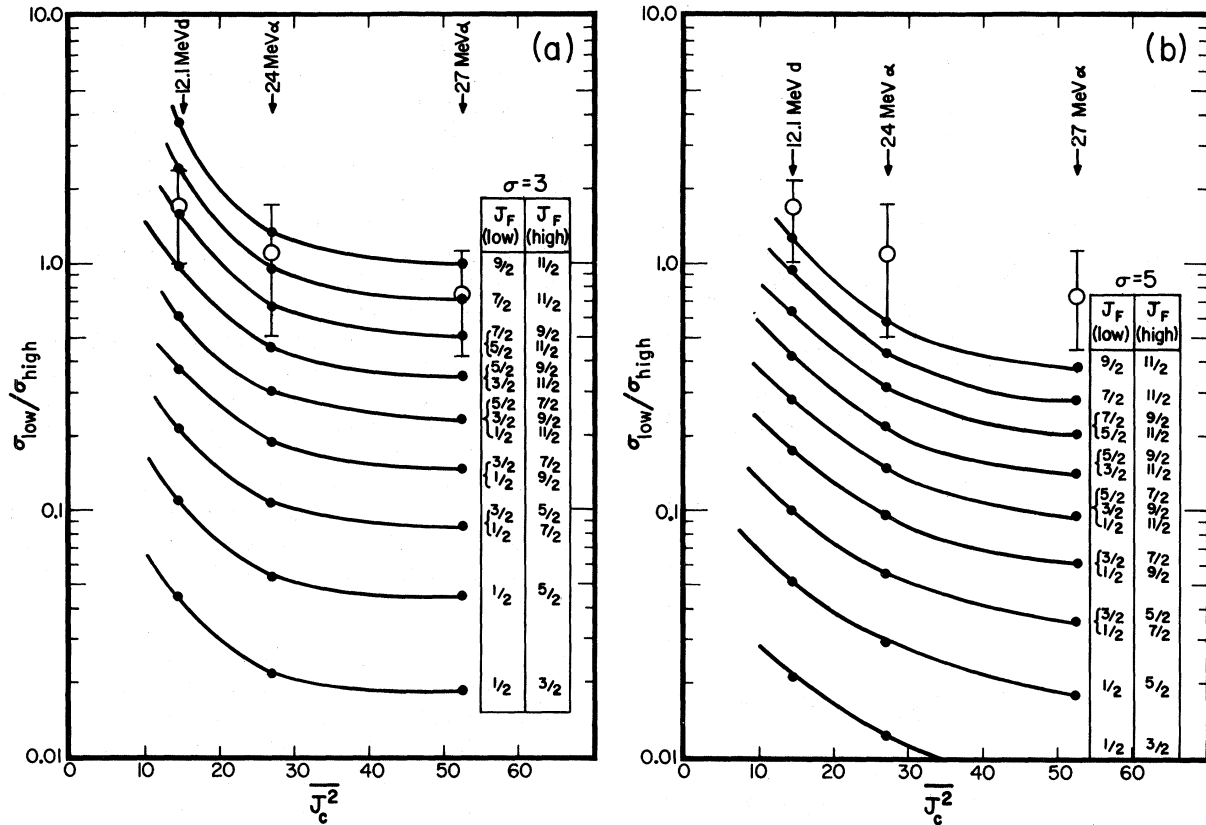


FIG. 6. Theoretical isomer production ratios for all final-state spin combinations between $\frac{1}{2}$ and $\frac{11}{2}$ as a function of the mean square initial compound-nuclear spin. Solid lines are drawn through the theoretical points corresponding to the spin pairs indicated at the right. The open circles are the experimental isomer ratios $\sigma_{\text{short}}/\sigma_{\text{long}}$. Theoretical calculations used spin cutoff parameters of (a) $\sigma=3$ and (b) $\sigma=5$.

lated to the different compound-nuclear angular momentum distributions.

A slight complication in the deduction of isomer spins from the calculations illustrated in Fig. 6 arises with consideration of the possibility of γ decay between the two states. The effect of this kind of γ branch depends on the relative energies of the two spin states. If the lower-spin state is the higher-energy state and decays partially by γ decay, the yield of the low-spin state is underestimated and the independent yield of the high-spin state is overestimated. Reference to Fig. 6 indicates that an increase in $\sigma_{\text{low}}/\sigma_{\text{high}}$ corresponding to a sizable γ branch is consistent only with the high-spin pairs $\frac{9}{2}, \frac{11}{2}$ and $\frac{7}{2}, \frac{11}{2}$. The existence of these spin pairs is unlikely for reasons discussed below and, therefore, the existence of this type of γ decay is improbable if the low-spin state is the higher-energy state. If the low-spin, short-lived state is the lower-energy state, the apparent experimental $\sigma_{\text{low}}/\sigma_{\text{high}}$ ratio again turns out to be an underestimate. This arises because the apparent yield of the long-lived isomer is virtually independent of whether it is observed via its fission

branch or via fission of the short-lived state, which is fed by the γ decay of the long-lived isomer and which comes into transient equilibrium with it. The independent yield of the short-lived isomer, however, is somewhat underestimated as the decay curve was resolved assuming no growth of the long-lived component.

Another mode of γ decay, that corresponding to penetration through the inner barrier and decay to the ground state, is in principle possible although such a decay mode has not been observed for any spontaneous fission isomer as yet. On the basis of the systematics of the dependence of the relative heights of the two barriers with mass number, this mode of decay is not expected to be large for plutonium isotopes but may be present in uranium and neptunium isotopes. If, however, the high-spin isomer decayed significantly by this mode (while the low-spin did not), the true isomer ratio $\sigma_{\text{low}}/\sigma_{\text{high}}$ would be lower than our experiment indicates and any spin pairs could be accommodated according to the calculations.

If then the statistical description of the population of the isomers is valid, and if preferential γ

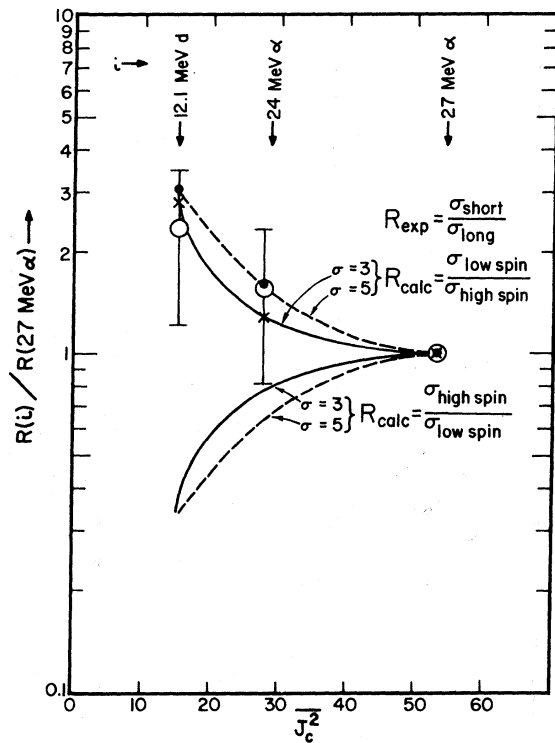


FIG. 7. Ratio of isomer ratio for each bombardment to the isomer ratio for the 27-MeV α -particle bombardment as a function of the mean square initial compound-nuclear spin. The open circles are the experimental results. The crosses connected by the solid line are the theoretical results for spin pairs $\frac{3}{2}, \frac{11}{2}$ and $\frac{5}{2}, \frac{9}{2}$ with $\sigma=3$. The solid points connected by the dashed line are theoretical results for the same spin pairs with $\sigma=5$. There is no error on the 27-MeV α -particle experimental point as this error has been propagated into the error of the ratio of isomer ratios for the other two points.

decay of the high-spin isomer through the inner barrier is assumed absent, the present analysis (Fig. 6) would limit the allowed spin pairs to $\frac{9}{2}, \frac{11}{2}$; $\frac{7}{2}, \frac{11}{2}$; $\frac{7}{2}, \frac{9}{2}$; and $\frac{5}{2}, \frac{11}{2}$; and possibly $\frac{5}{2}, \frac{9}{2}$ and $\frac{3}{2}, \frac{11}{2}$. These can be further limited by the available Nilsson single-particle levels in the deformation re-

gion of ^{237m}Pu . A brief survey of the Nilsson levels near the Fermi surface for 143 neutrons ($A=242$)²¹ at deformations between $\epsilon=0.60$ and 0.70 ($\epsilon_4=0.04$) shows that for excited neutron particle or hole states, the possible spin pairs within 1 MeV of the Fermi surface do not include the pairs $\frac{7}{2}, \frac{11}{2}$; $\frac{7}{2}, \frac{9}{2}$; $\frac{5}{2}, \frac{9}{2}$; and $\frac{9}{2}, \frac{11}{2}$. It is reasonable to exclude the existence of a three-quasiparticle neutron state or a two-quasiparticle proton state, since the final states involved are likely to be very high-spin states for which the cross sections for the 12.1-MeV deuteron bombardment would be much lower than this experiment indicates. The most probable spin pairs corresponding to the short- and long-lived components are therefore $\frac{5}{2}, \frac{11}{2}$ and possibly $\frac{3}{2}, \frac{11}{2}$. The former two spin states cross at a deformation of $\epsilon=0.62$ and the latter two at $\epsilon=0.64$ in the diagram²¹ with $\epsilon_4=0.04$. In a slightly different diagram²² corresponding to a continuous variation of ϵ_4 with ϵ the respective crossing points are $\epsilon=0.61$ and $\epsilon=0.59$. The steepness of the energy of the $\frac{11}{2}^- [505]$ single-particle state with deformation results in a quite narrow region of deformation for which this state lies close to the Fermi surface. Assuming that its position is well determined in the level scheme (it has been observed at ground-state deformations in the rare earth region^{23, 24}) and that the Nilsson diagram is valid at these deformations, the present results indicate the deformation of the second minimum to be approximately 0.6. This is in good agreement with the calculations of Nilsson *et al.*²¹ This $\frac{11}{2}^-$ single-particle state has been proposed²² as the origin of a possible long-lived isomer in ^{241}Pu , although the existence of this isomer has not been confirmed.

ACKNOWLEDGMENTS

We are very grateful to Dr. Sven Bjørnholm for calling to our attention the implications of γ decay of the long-lived isomer to the short-lived isomer on the deduced isomer ratio.

†Work supported in part by the U. S. Atomic Energy Commission.

*Present address: Bhabha Atomic Research Centre, Trombay-Bombay, India.

‡Present address: Argonne National Laboratory, Argonne, Illinois.

¹V. M. Strutinsky, Nucl. Phys. **A122**, 1 (1968).

²S. Bjørnholm and V. M. Strutinsky, Nucl. Phys. **A136**, 1 (1969).

³R. Vandenbosch and K. L. Wolf, in *Proceedings of the Second International Atomic Energy Symposium on Physics and Chemistry of Fission, Vienna, Austria, 1969*

(International Atomic Energy Agency, Vienna, Austria, 1969).

⁴S. C. Burnett, H. C. Britt, B. H. Erkkila, and W. E. Stein, Phys. Letters **31B**, 523 (1970).

⁵J. E. Lynn, in *Proceedings of the Second International Atomic Energy Symposium on Physics and Chemistry of Fission, Vienna, Austria, 1969* (International Atomic Energy Agency, Vienna, Austria, 1969).

⁶K. L. Wolf, Ph.D. thesis, University of Washington, 1969 (unpublished).

⁷J. O. Newton, Progr. Nucl. Phys. **4**, 234 (1955).

⁸D. L. Hill and J. A. Wheeler, Phys. Rev. **89**, 1102 (1953).

- ⁹H. Fauska, N. G. Ward, J. Lilley, and C. F. Williamson, *Nucl. Instr. Methods* **63**, 93 (1968).
- ¹⁰K. L. Wolf, R. Vandenbosch, P. A. Russo, M. K. Mehta, and C. R. Rudy, *Phys. Rev. C* **1**, 2096 (1970).
- ¹¹R. Vandenbosch, T. D. Thomas, S. E. Vandenbosch, R. A. Glass, and G. T. Seaborg, *Phys. Rev.* **111**, 1358 (1958); J. Wing, W. J. Ramler, A. L. Harkness, and J. R. Huizenga, *ibid.* **114**, 163 (1969).
- ¹²S. Björnholm, I. Borggreen, Yu P. Gangrskii, and G. Sletten, *Yadern Fiz.* **8**, 470 (1968) [transl.: *Soviet J. Nucl. Phys.* **8**, 267 (1969)].
- ¹³S. M. Polikanov and G. Sletten, *Nucl. Phys.* **A151**, 656 (1970).
- ¹⁴J. R. Huizenga and R. Vandenbosch, *Phys. Rev.* **120**, 1305 (1960).
- ¹⁵R. Vandenbosch and J. R. Huizenga, *Phys. Rev.* **120**, 1313 (1960).
- ¹⁶W. L. Hafner, Jr., J. R. Huizenga, and R. Vandenbosch, Argonne National Laboratory Report No. ANL-6662, 1962 (unpublished).
- ¹⁷The optical-model parameters used for α particles are those given by J. R. Huizenga, R. Vandenbosch, and H. Warhanek in *Phys. Rev.* **124**, 1964 (1961), and for deuterons those given by G. L. Bate, R. Chaudhry, and J. R. Huizenga, *Phys. Rev.* **131**, 722 (1963).
- ¹⁸D. Vinciguerra and K. Kotajima, *Nucl. Phys.* **77**, 347 (1966).
- ¹⁹S. K. Mangal and C. S. Khurana, *Nucl. Phys.* **69**, 158 (1965).
- ²⁰J. H. Carver, G. E. Coote, and T. R. Sherwood, *Nucl. Phys.* **37**, 449 (1962).
- ²¹S. G. Nilsson, C. F. Tsang, A. Sobiczewski, Z. Szymanski, S. Wycech, C. Gustafson, I. Lamm, P. Möller, and B. Nilsson, *Nucl. Phys.* **A131**, 1 (1969).
- ²²S. G. Nilsson, G. Ohlen, C. Gustafson, and P. Möller, *Phys. Letters* **30B**, 437 (1969).
- ²³J. Borggreen, H. J. Frahm, N. J. Sigund Hansen, and S. Björnholm, *Nucl. Phys.* **72**, 509 (1965).
- ²⁴J. Borggreen and G. Sletten, *Nucl. Phys.* **A143**, 255 (1970).

PHYSICAL REVIEW C

VOLUME 3, NUMBER 4

APRIL 1971

Angular Correlation of Gamma Cascades in Gd^{155} , and Levels of Gd^{155} Populated by the Decay of $\text{Tb}^{155\ddagger}$

H. Bakhru

Yale University, New Haven, Connecticut 06520 and State University of New York, Albany, New York 12203

and

S. Shastry

State University of New York, Plattsburgh, New York 12901 and Yale University, New Haven, Connecticut 06520

and

J. Boutet*

Yale University, New Haven, Connecticut 06520

(Received 6 July 1970)

The level scheme of Gd^{155} has been studied using high-resolution $\text{Ge}(\text{Li})$, $\text{Si}(\text{Li})$, and standard scintillation counters. The analysis of the experimental data for this nucleus is impeded by an ambiguity in the spin values of the majority of its excited states. In the present work γ - γ angular correlations in the decay of Tb^{155} - Gd^{155} were measured using a $\text{Ge}(\text{Li})$ detector in coincidence with $\text{NaI}(\text{Tl})$ scintillation counter. The spins of some of the levels up to the 648.1-keV level have been confirmed from various cascades. The analysis of the various coincidence experiments leads to the proposal of levels in Gd^{155} at 60.0, 85.5, 105.3, 118.0, 146.0, 235, 266.6, 268.6, 286.8, 326.0, 367.7, 427.4, 451.3, 488.8, 559.9, 592.6, 615.5, and 648.1 keV. A consistent level scheme of Gd^{155} is proposed and the spin and parity assignments of the levels are discussed. The multipolarity of the different γ rays including the percentage of mixing is reported.

I. INTRODUCTION

The Gd^{155} nucleus has recently been the object of intensive experimental investigation. The nuclear energy levels have been studied by stripping and pick-up reactions,^{1,2} by radioactive decay work,³⁻⁶ by Coulomb excitation,⁷ and by Mössbauer spectroscopy.^{8,9} The neighboring odd- N nucleus Gd^{157} is "well behaved" in the sense that almost

all the levels and their properties can be described by one corresponding Nilsson state. Although, there is considerable evidence that Gd^{155} , at least in its ground state, is strongly deformed ($\delta = 0.3$),¹⁰ a satisfactory description of the lowest-lying positive-parity states in this nucleus has not previously been given, in spite of the large amount and wide variety of experimental data that exist concerning them. The main problem is due to the